

## **ELECTRICAL ENGINEERING**

### **Attenuation and EMI Frequency Spectrum for Distribution Lines**

**A.H.Al-Bahrani and N.H.Malik**

*Department of Electrical Engineering, College of Engineering, King Saud University,  
P.O. Box 800, Riyadh-11421, Saudi Arabia*

**Abstract.** Corona and gap discharges occur at discrete points on distribution lines. Such discharges may produce electromagnetic interference (EMI) to the communication and control systems operating near such lines. Due to the discrete nature of distribution lines EMI sources, the total EMI produced by them is strongly influenced by the attenuation characteristics of the line. This paper discusses the factors which can influence the attenuation characteristics of distribution lines. Attenuation values are calculated for a typical three phase distribution line for different values of frequency, earth resistivity, conductor size, inter-conductor spacing, height and ground wire arrangement. The resulting values are presented in the form of empirical equations. Using such attenuation values, the relationship between the injected and measured noise is discussed for isolated as well as uniformly distributed noise sources. It is shown that unlike transmission lines, the distribution lines EMI may exhibit a variety of EMI frequency spectra depending upon the lines and soil parameters, type of noise source, as well as location of measurement point with respect to the noise source.

#### **Introduction**

Corona and gap discharges occur on high voltage transmission and distribution lines. Such discharges can result in electromagnetic interference (EMI) to the communication and control systems which operate near these lines. Therefore, the EMI characteristics of transmission and distribution lines are of significant practical interest.

The EMI characteristics of EHV and UHV transmission lines have been extensively studied in the past due to increasing use of such lines [1–8]. The major EMI source on transmission line is the conductor corona which occurs roughly uniformly over the entire length of the line. Consequently, the EMI frequency spectrum observed at any point along the transmission line reflects upon the frequency spec-

trum of the EMI source *i.e.* the corona current pulses. Distribution lines, on the other hand, usually have low operating gradients. Consequently, such lines do not have a general conductor corona. However, corona can occur at discrete points produced by poor construction procedures. Moreover, gap discharges as well as discharges on insulators can occur due to man made as well as naturally produced defects. As a result, distribution lines can generate appreciable levels of EMI as shown in [8]. This is specially true for lines which are located in arid desert lands where insulator contamination problem can become severe, thereby, increasing interference from the insulators. Figs 1 and 2 show EMI levels measured under 380 KV transmission lines and 33 KV distribution lines located in the Central Region of Saudi Arabia. As seen here, the distribution lines EMI levels are even higher than those of the transmission lines.

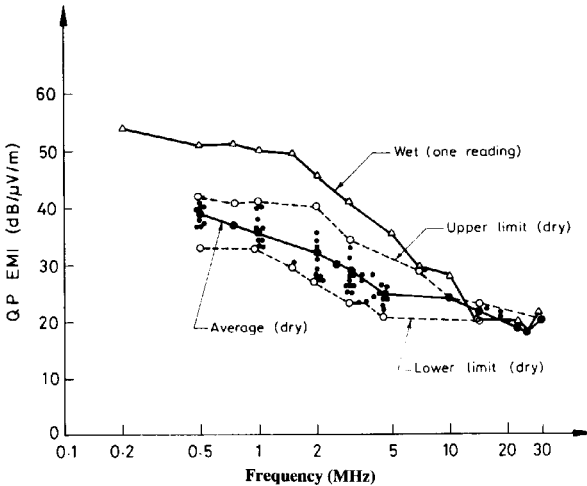


Fig. 1. EMI levels measured under 380 KV transmission lines, taken from [8]

Unlike transmission lines, the distribution lines EMI sources are usually located at poles. The injected noise undergoes attenuation as it propagates along the line. Consequently, the EMI frequency spectrum measured at any point along the line may or may not reflect on the frequency spectrum of the EMI source itself. This is due to the fact that, besides other factors, the EMI attenuation strongly depends upon frequency. Therefore, the frequency dependence of attenuation characteristics of distribution lines are of significant practical interest. A review of the available literature indicates a general lack of such information.

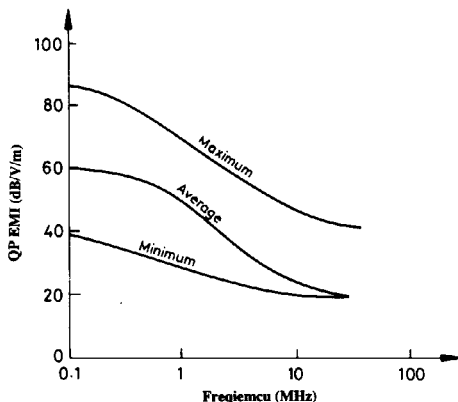


Fig. 2. EMI levels measured under 33 KV distribution lines, taken from [8]

This paper examines in detail, the attenuation characteristics of distribution lines. The influence of conductor size, its height as well as spacing, frequency, ground resistivity and arrangement of earth wire on the attenuation characteristics of such lines is examined. Furthermore, the effect of attenuation on the EMI frequency spectrum of such lines is considered for isolated as well as uniformly distributed EMI sources, and it is shown that for distribution lines, the measured frequency spectrum may or may not reflect on the nature of the EMI source.

### General Line Equations

Three-phase overhead lines may have bundle conductors and/or ground wires. The voltages and currents along all  $n$  parallel conductors are related in the frequency domain by:

$$-\frac{d[V(x,\omega)]}{dx} = [Z(\omega)][I(x,\omega)] \quad (1)$$

$$-\frac{d[I(x,\omega)]}{dx} = j\omega [C][V(x,\omega)] \quad (2)$$

The elements of the symmetric series  $n \times n$  impedance matrix  $[Z(\omega)]$  in Eq. (1) are frequency dependent due to the skin effect of the ground return and of the con-

ductors themselves. These elements are usually calculated from Carson's formula [9], or from much simpler impedance formulas with closed form solution which have recently been developed [10, 11].

The elements of the constant real  $n \times n$  capacitance matrix  $[C]$  in Eq. (2) are obtained indirectly, by building a "potential coefficient" matrix  $[P]$  and then inverting it to get  $[C]$ . [12]

The resulting  $n$  equations for all conductors will contain more information than is usually needed. Generally, only the phase variables are of interest. The original system may be reduced by matrix reduction techniques to a one conductor per phase equivalent system. This reduction is performed by eliminating ground wires and by bundling of conductors [12]. However, their effects are reflected in the equivalent impedances and admittances of the reduced system.

Equations (1) and (2) may be used to describe a three-phase reduced system if  $[V(x,\omega)]$  and  $[I(x,\omega)]$  represent vectors of phase voltages and currents along the line, and  $[Z(\omega)]$  and  $[C]$  are the reduced  $3 \times 3$  impedance and capacitance matrices. From Eqs. (1) and (2), the following wave equations may be obtained:

$$\frac{d^2 [V(x,\omega)]}{dx^2} = j\omega [C][Z(\omega)][V(x,\omega)] \quad (3)$$

$$\frac{d^2 [I(x,\omega)]}{dx^2} = j\omega [Z(\omega)][C][I(x,\omega)] \quad (4)$$

Equations (1) to (4) are coupled differential equations with frequency dependent coefficients. These equations may be decoupled, however, through modal transformation [13]. Each component of the new modes may be individually analyzed as a single phase line.

Assuming that  $Z'(\omega)$  and  $Y'(\omega)$  denote the per unit length series impedance and shunt admittance for any one of the three modes respectively, then the corresponding modal propagation constant is defined as:

$$\gamma = \alpha' + j\beta = \sqrt{Z'(\omega)Y'(\omega)} \quad (5)$$

Therefore, the attenuation  $\alpha$ , in db/unit length, is given by:

$$\alpha = 20\alpha' \log(e) = 8.6859\alpha' \quad (6)$$

## Results and Discussion

### Attenuation

Fig. 3 shows schematic of a 33 KV three-phase distribution line of a horizontal configuration used for the present analysis. The phase conductors are assumed to be ACSR Pelican of 477,000 CMIL area and 20.7 mm diameter. The earth wire is galvanized steel conductor of 7.9 mm diameter. The average height of conductors above ground is 8 m. Fig. 4 shows the variation of modal attenuations for this line for an earth resistivity value ( $\rho$ ) of 100  $\Omega$ -m. In these calculations it was assumed that ground or earth wire is continuously grounded at each pole. It is clear from Fig. 4 that, as expected, ground mode has the highest attenuation where as the attenuation of line mode 1 (bipolar mode) and line mode 2 (interphase mode) are more or less similar with mode 1 having slightly higher attenuation values. The modal attenuations  $\alpha$  in db/km as shown in Fig. 4 can be approximated by equations of the following form:

$$\alpha = Kf^n \quad (7)$$

where K (db/km MHz) and n are constants and f is frequency in MHz. The values of constants K and n are different for different modes. For the data shown in Fig. 4. The values of these constants are given in the following table:

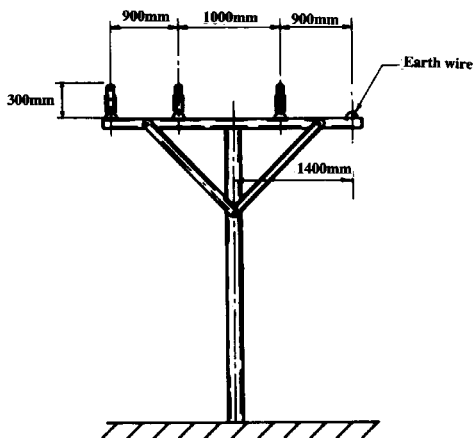


Fig. 3. 33 KV Distribution line configuration

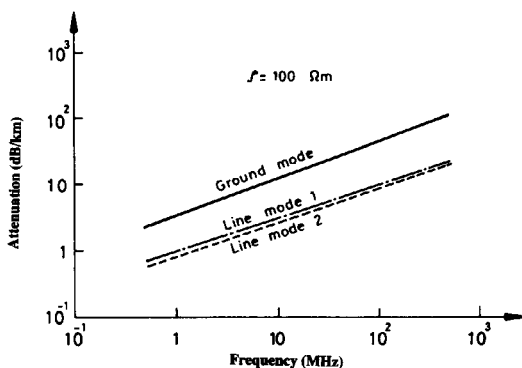


Fig. 4. Modal attenuations

| Mode        | K      | n      |
|-------------|--------|--------|
| ground mode | 3.4232 | 0.5589 |
| line mode 1 | 0.9636 | 0.5026 |
| line mode 2 | 0.8078 | 0.5163 |

### Effect of earth resistivity

For a given distribution line, the values of K and n corresponding to the ground mode strongly depend upon  $\rho$ . For modes 1 and 2, the ground resistivity ( $\rho$ ) also has some minor influence on the values of K and n. For the line shown in Fig. 3  $\alpha$  for the various modes was computed for different values of  $\rho$  and f. It was found that  $\alpha$  can be expressed as follows over the range of  $0.5 \leq f \leq 500$  MHz and  $50 \leq \rho \leq 2000$   $\Omega$ -M.

a) *Ground mode*

$$\alpha = \{ 0.93 \ln(\rho) - 0.86 \} f^{0.4} \rho^{0.072} \quad (8)$$

b) *Line mode 1*

$$\alpha = 1.011 \rho^{-0.011} f^{0.51} \rho^{-0.0007} \quad (9)$$

c) *Line mode 2*

$$\alpha = 0.77 \rho^{0.01165} f^{0.438} \rho^{0.0361} \quad \text{for } 50 \leq \rho \leq 400 \text{ } \Omega\text{-m} \quad (10)$$

and

$$\alpha = 0.8846 \rho^{-0.0103} f^{0.438} \rho^{0.0361} \quad \text{for } 400 < \rho \leq 2000 \text{ } \Omega\text{-m} \quad (11)$$

It is obvious from Eqs. (8) to (11) that the effect of frequency as well as earth resistivity is different for each mode.

### Effect of earth wire segmentation

Equations (8) to (11) are applicable for the case where the earth wire is continuously grounded at each pole. Some times, the earth wire is segmented, *i.e.* the earth wire is grounded in the middle, and is insulated at the adjacent poles to the right and left. At both ends of the segmentation section, the earth wire is interrupted as well, to prevent circulating currents. Segmented earth wires are handled in the line parameters calculations by ignoring them in the series impedance calculation, and taking them into account only in the calculation of the capacitances.

The calculations were also made for the line of Fig. 3 but assuming segmented earth wire. The resulting attenuation values can best be described by the following equations over the previously mentioned ranges of  $f$  and  $\rho$  values.

a) *Ground mode*

$$\alpha = \{2.2023 \ln(\rho) - 3.9572\} f^{0.415} \rho^{0.0633} \quad (12)$$

b) *Line mode 1*

$$\alpha = 0.9712 \rho^{0.0125} f^{0.4061} \rho^{-0.0561} \quad \text{for } 50 \leq \rho \leq 200 \Omega - \text{m} \quad (13)$$

and

$$\alpha = (-2.3971 \times 10^{-5} \rho + 1.0452) f^{0.4061} \rho^{-0.0561} \quad \text{for } 200 \leq \rho \leq 2000 \Omega - \text{m} \quad (14)$$

c) *Line mode 2*

$$\alpha = 0.8775 \rho^{0.1453} f^{0.4867} \rho^{0.0117} \quad \text{for } 50 \leq \rho \leq 400 \Omega - \text{m} \quad (15)$$

and

$$\alpha = 0.8491 f^{0.4867} \rho^{0.0117} \quad \text{for } 400 \leq \rho \leq 2000 \Omega - \text{m} \quad (16)$$

A comparison of  $\alpha$  values for continuously grounded and segmented earth wire indicates that segmented earth wire produces considerably higher attention values for all modes. This difference is influenced by the frequency as well as earth resistivity values and is specially pronounced for ground mode as well as for line mode 1. For line mode 2, the influence of earth wire segmentation is less pronounced.

It is important to mention that Eqs. (8)–(16) are strictly applicable for earth resistivity values in the range of 50–2000  $\Omega$ -m which covers most of the soils that are of practical interest. However, soil resistivity can be as low as a few milli-ohms-m (salt water saturated-soil near the sea) and as high as a few kilo-ohms-m (rock salt and

ice). The application of Eqs. (8)–(16) to such extreme values of  $\rho$  may lead to significant errors in the  $\alpha$  values.

### Effect of conductor size

Conductor size can also influence the values of  $\alpha$ . The above mentioned values of  $\alpha$  are for ACSR conductor of 477,000 CMIL area. Calculations were also performed for the line configuration shown in Fig. 3 but for different conductor sizes. It was observed that, as expected, ground mode attenuation is not affected by the phase conductor size. However, the attenuation of line modes 1 and 2 are affected by the phase conductor size. For both of these modes, the general tendency is that  $\alpha$  will increase when conductor cross sectional area becomes smaller. The extent of increase is slightly different for line modes 1 and 2. Let  $R_1$  be the ratio of modal attenuation  $\alpha$  for ACSR conductor of area A (CMIL) to that of an ACSR conductor of area 477,000 CMIL at a given frequency *i.e.*

$$R_1 = \frac{\alpha \text{ for A (CMIL)}}{\alpha \text{ for 477,000 (CMIL)}} \quad (17)$$

It is observed that  $R_1$  is more or less independent of the frequency. If  $R_2 = A/477,000$ , then for conductors with size in the range of  $266,800 \leq A \leq 1,272,000$ ,  $R_1$  and  $R_2$  are related by

$$R_1 = R_2^{-m} \quad (18)$$

where  $m = 0.3934$  for line mode 1 and  $m = 0.3714$  for line mode 2. Thus combining the above equation and the equation for the appropriate modal attenuation as given earlier, it is possible to estimate  $\alpha$  values for any conductor size for the line configuration shown in Fig. 3.

### Effect of conductor spacing

For the same conductor size,  $\alpha$  values were calculated by using different values of interconductor spacings for the line of Fig. 3. The results showed that  $\alpha$  values for modes 1 and 2 are not affected very much by the inter-conductor spacings. However, the attenuation for ground mode decreases when conductor spacing is increased. Fig. 5 shows the attenuation values for the configuration of Fig. 3 and for the case when the inter-conductor spacings are five times the values shown in Fig. 3, where the other parameters are kept the same. It is clear from Fig. 5, that the decrease in the  $\alpha$  values for the ground mode depends upon frequency and it is in the range of 15 to 25%.

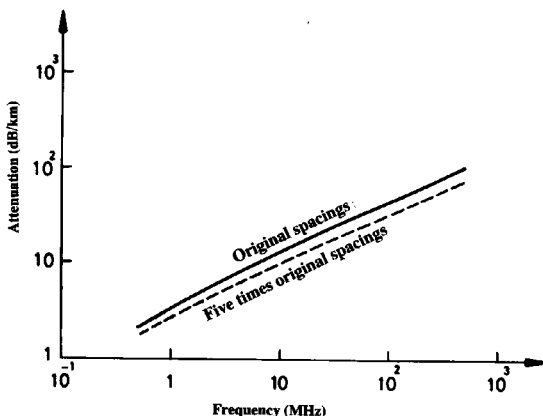


Fig. 5. Effect of spacing on ground mode attenuation

### Effect of line height

If the line height is increased while the other parameters are kept the same, the  $\alpha$  values decrease for all three modes. However, the percentage decrease is the highest for line mode 1 while it is the lowest for the ground mode. The results for  $\rho = 100 \Omega\text{-m}$  showed that, if the conductor heights in Fig. 3 are doubled, the  $\alpha$  values are decreased by 40 to 55% for the ground mode, and 1 to 5% for line mode 2. There was no change in the  $\alpha$  values for line mode 1. The highest decrease is at the highest frequency.

### Significance of Attenuation Values

The results in the previous section indicate clearly that the EMI attenuation increases with increasing frequency and ground resistivity values. Furthermore, it increases when the conductor size, conductor height above ground, as well as inter-conductor spacings are decreased. The net result is that distribution lines will have higher attenuation values as compared to transmission lines since the distribution lines have low heights and have conductors close to each other. Furthermore, since the phase conductors of distribution lines are relatively close to each other, the interference field produced at the ground level is due only to the line to ground mode, other modes (*i.e.* line modes 1 and 2) being negligible [2]. Therefore, for distribution lines, ground mode attenuation values are of great significance. For distribution lines located mainly in hot, dry, desert lands, such as the Central Region of Saudi Arabia, the attenuation values become excessively high due to very large values of earth

resistivity for such soils. It is well known that dry sandy, loamy soil can have earth resistivity values in the range of 100 to 10,000  $\Omega$ -m. For a given value of earth resistivity, the attenuation of a single phase line is approximately similar to the ground mode attenuation value of a three-phase line having similar conductor height as well as size. Thus, one can use equations (8) and (12) to discuss the influence of attenuation values on EMI characteristics. In order to examine such an influence, the characteristics of EMI sources normally found on distribution lines will be discussed next.

#### **Distribution line EMI sources**

The EMI on distribution lines is generated by [2]:

- a) corona,
- b) gap-type discharges.

The frequency spectrum of corona current pulses is determined by the physical discharge mechanism and is not influenced by impedance in external circuit that delivers the high voltage. Therefore, the frequency spectrum of a particular type of corona discharge can be considered to be characteristic of that type of discharge. For AC power lines, the interference is primarily due to positive corona pulses.

Gap-type discharges occur at small gaps with sufficient voltage gradients. The current pulse shape of the discharge is not determined by the discharge itself but by the external circuit and the gap capacitance. Therefore, the gap discharge current waveform can vary from one case to the next. The types of gap discharges which can occur on distribution lines are:

- a) *Sparks between two metal parts*, such as between cap and pin in insulator string, at the connection of insulator to the tower or the line conductor and bad contacts between metal parts.
- b) *Micro-sparks* between metal parts and electrically charged insulating surface.
- c) *Surface discharges* on insulators.

A typical frequency spectrum of a corona current pulse and an example of the spectrum of a gap-type discharge are given in Figs. 6 and 7 respectively ( $x = 0$  cases) [2], which represent the spectra of the injected noise into the power lines.

#### **Isolated EMI source**

It is clear from the above discussion that the gap-type discharge sources on distribution lines will occur at poles. Furthermore, since operating gradients are low for

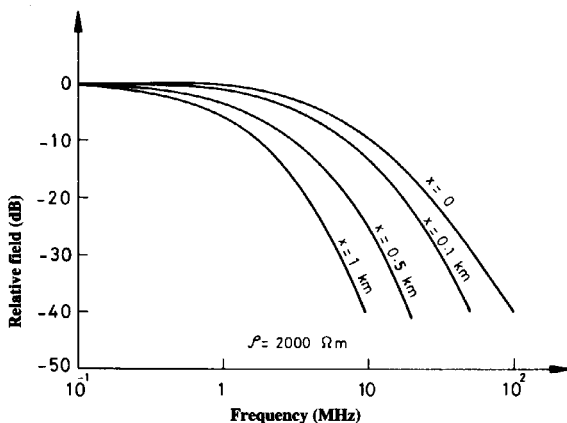


Fig. 6. Variation of the corona noise field

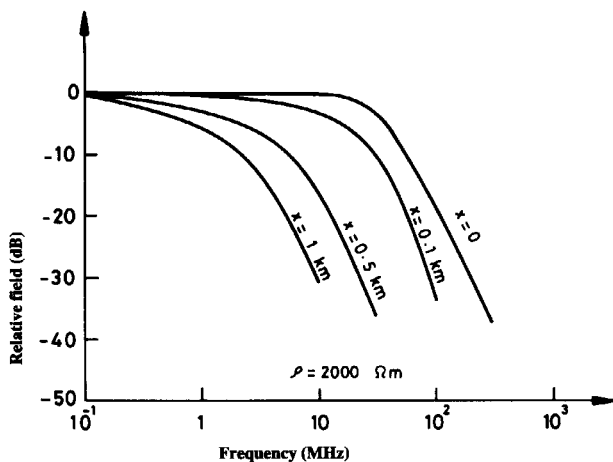


Fig. 7. Variation of the gap-discharge noise field

such lines, corona can only occur at sharp points left on the line (e.g. a projecting tie wire used to connect the conductor to the cap of an insulator, etc). Such sharp points will also be generally located on poles. Therefore, the EMI sources on distribution

lines in general, will be randomly located at poles. As the worst case, there will be such sources at each pole. First let us consider a single isolated EMI source (either a corona or a gap discharge) which produces noise field of  $N_0(f)$  on both sides of the injection point. If  $\alpha'(f)$  is the attenuation constant (nepers/unit length), then  $N_x(f)$ , the noise field at distance  $x$  from the source is given by:

$$N_x(f) = N_0(f)e^{-\alpha'(f)x} \quad (19)$$

Figures 6 and 7 show the calculated values of  $N_x(f)$ , at  $x = 0.1, 0.5,$  and  $1$  Km from the injection point, for corona and a gap discharge for  $\rho = 2000 \Omega\text{-m}$  respectively. These figures also show  $N_0(f)$ , ( $x = 0$  cases), for both types of noise sources. It is clear from these figures, that for frequencies above 10 MHz, even at 100 m distance from the injection point, there are significant differences between  $N_x(f)$  and  $N_0(f)$ , and only for frequencies below 10 MHz, the difference between two values is less than 3 db. Consequently, the higher frequency interference components will be quickly attenuated below the background noise level if the EMI measurements are performed at a location which is even a few spans away from the noise source. Therefore, based upon EMI frequency measurements, one can differentiate between a corona source and a gap discharge noise source only if the EMI measurements are performed near (*i.e.*  $\approx$  less than 100 m distance from) the random EMI source.

### Regularly distributed EMI sources

From the above discussion, it is obvious that it may or may not be possible to identify a random EMI source based upon random EMI frequency spectrum measurements. In this section we will discuss the influence of attenuation of the EMI if similar sources are regularly distributed along a single phase line which is infinitely long on both sides of the observation point located at mid span. The total noise  $N(f)$  at the observation point will be due to the quadratic summation of the individual noise components arriving from both sides of the observation point. Thus

$$\begin{aligned} N^2(f) &= 2N_0^2(f)e^{-\alpha'(f)s} + 2N_0^2(f)e^{-3\alpha'(f)s} + 2N_0^2(f)e^{-5\alpha'(f)s} + \dots \\ &= 2N_0^2(f)e^{-\alpha'(f)s} [1 + e^{-2\alpha'(f)s} + e^{-4\alpha'(f)s} + \dots] \end{aligned} \quad (20)$$

where  $s$  = span length. This can be simplified to

$$N(f) = \sqrt{2}N_0(f) \left[ \frac{e^{-0.5\alpha'(f)s}}{\sqrt{1 - e^{-2\alpha'(f)s}}} \right] \quad (21)$$

It is clear from this equation that the shape of the spectrum of the injected noise  $N_0(f)$  will be different from the shape of the spectrum of the noise observed at the mid span. (i.e.  $N(f)$ ) due to the frequency dependence of the attenuation i.e.  $\alpha'(f)$ . In Eq. (21), the term within the square brackets represents the attenuation/amplification of the noise. At low frequencies,  $\alpha'(f)$  will be small. Consequently,  $e^{-2\alpha'(f)s}$  will be slightly less than 1. Therefore, the term within the square root will be very small. Hence, the term within the square brackets will be more than 1. This will give an overall amplification which physically implies that the noise  $N(f)$  will be due to many sources on both sides of the observation point. At the high end of the frequency where  $\alpha'(f)$  has very large values, the term within the square root will approach 1. Thus, the term within the square brackets will be less than 1 resulting in an overall attenuation with respect to the injected noise. Fig. 8 shows a plot of the attenuation/amplification factor i.e. the term within the square brackets of Eq. (21), for  $\rho = 2000 \Omega\text{-m}$  and continuously grounded earth wire. It is clear from this figure that this factor is zero at the cross-over frequency  $f_c \approx 15 \text{ MHz}$ . If  $\rho$  is large or ground wire is segmented, this cross-over frequency will become lower. The net result will be that such distribution lines will exhibit significant noise at low frequencies but noise will diminish very rapidly with frequency especially if the noise sources are corona discharges. Actual EMI measurements on distribution lines in the Central Region of Saudi Arabia verify this behavior [8].

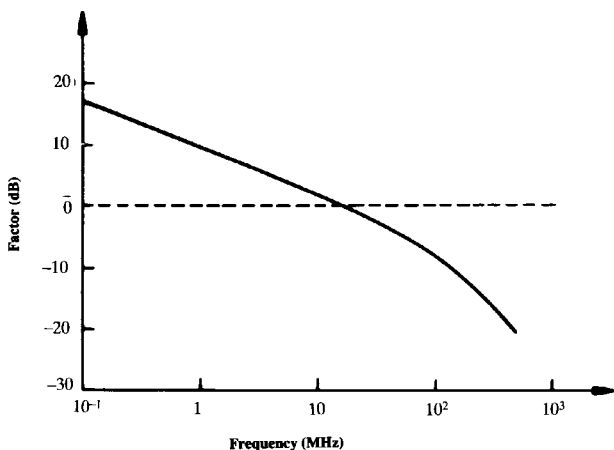


Fig. 8. Variation of the attenuation/amplification factor

#### 4. Conclusions

The attenuation of distribution lines are influenced by frequency, line design as well as soil parameters. The attenuations of different modes vary according to a power law of the form  $\alpha = Kf^n$  where K and n depend upon type of mode. Ground mode has the highest attenuation which strongly depends upon earth resistivity. Empirical equations are derived for modal attenuation values for a wide range of parameters.

The EMI characteristics of distribution lines strongly depend upon the attenuation values for isolated as well as uniformly distributed noise sources. The measured frequency spectra for such lines may or may not reflect on the nature of EMI source as usually assumed.

#### References

- [1] Laforest, J.J. *Transmission Line Reference Book – 345 KV and Above*. 2<sup>nd</sup> Ed. U.S.A. California: EPRI, 1982.
- [2] CIGRE Committee Report Prepared by Working Group 36.01, "Interference Produced by Corona Effect of Electric Systems: Description of Phenomena, practical Guide for Calculation." *Electra*, Paris, France, (1974).
- [3] IEEE Committee Report. "CIGRE/IEEE Survey on Extra High Voltage Transmission Line Radio Noise." *IEEE Transaction on Power Apparatus and Systems*, Vol. PAS-92 (1973), pp. 1019-1028.
- [4] IEEE Committee Report. "Radio Noise Design Guide for High Voltage Transmission Lines." *IEEE Transaction on Power Apparatus and Systems*, Vol. PAS-90 (1971) pp.833-843.
- [5] Moreau, M.R. and Gary, C.H. "Predetermination of Radio Interference Level of High Voltage Lines, Part I and II." *IEEE Transaction on Power Apparatus and Systems*, Vol. PAS-91 (1972), pp. 284-304.
- [6] CIGRE Report. "Comparison of Radio Noise Prediction Methods with CIGRE/IEEE Survey Results." *Electra*, No. 22 (1972).
- [7] Al-Arainy, A.A.; Malik, N.H. and Abdul-Aal, L.N. "Electromagnetic Interference from Transmission Lines Located In Central Region of Saudi Arabia." *Winter Power Meeting in New York, IEEE Paper No. 88 WM 062-2* (1988).
- [8] Al-Arainy, A.A.; Malik, N.H. and Abdul-Aal, L.N. "Electromagnetic Interference from Power Lines in Central Region of Saudi Arabia." *Final Report for KACST Project AR-6-38*, Riyadh, Saudi Arabia, Dec. (1988).
- [9] Carson, J.R. "Wave Propagation in Overhead Wires with Ground Return." *Bell System Techn. Journal*, 5 (1962), 539-554.
- [10] Deri, A.; Tevan, G.; Symlyen, A. and Castanheira, A. "The Complex Ground Return Plane, a Simplified Model for Homogeneous and Multi-layer Earth Return." *IEEE Transaction on Power Apparatus and Systems*, Vol. PAS-100, Aug. (1981), pp. 3686-3693.
- [11] Alvarado, F.L. and Betancourt, R. "An Accurate Closed-Form Approximation for Ground Return Impedance Calculations." *Proceeding of IEEE*, Vol. 71, No. 2, Feb. (1983), pp. 279-280.
- [12] Dommel, H.W. "Overhead Line Parameters from Handbook Formulas and Computer Programs." *IEEE Transaction on Power Apparatus and Systems*, Vol. PAS-104, Feb. (1985), pp.366-372.
- [13] Hedman, D.E. "Propagation of Overhead Transmission Lines: I - Theory of Modal Analysis, II - Earth-Conduction Effects and Practical Results." *IEEE Transaction on Power Apparatus and Systems*, Vol. PAS-84. March (1985), pp.200-211.

## الوهن وطيف تردد التداخلات الكهرومغناطيسية لخطوط التوزيع الكهربائية

عبدالله حسين البحراني ونذر حسين مالك

قسم الهندسة الكهربائية، كلية الهندسة، جامعة الملك سعود، ص.ب ٨٠٠،  
الرياض ١١٤٢١، المملكة العربية السعودية

ملخص البحث . تحدث التفريغات التاجية والانهارات الفجوية عند نقاط منفصلة على خطوط التوزيع الكهربائية التي قد تسبب في حدوث موجات ذات ترددات عالية ينتج عنها تداخلات في أجهزة الاتصال والتحكم القريبة . هذه التداخلات الكهرومغناطيسية تتأثر كثيرا بخاصية الوهن لكل خط وذلك بسبب الطبيعة المنفصلة لمصدرها .

يناقش هذا البحث العوامل المؤثرة في خاصية الوهن في خطوط التوزيع الكهربائية، حيث تم حساب قيم الوهن لخط مثالي ثلاثي الطور لقيم مختلفة لكل من: التردد، المقاومة النوعية للتربة، حجم الموصلات والمسافات الفاصلة بينها وارتفاعها عن الأرض بالإضافة إلى أشكال مختلفة لسلك التأريض . ولقد أبرزت القيم الناتجة على شكل معادلات نوقشت من خلالها العلاقة بين مصادر التشويش والتشويش المقاس لمصدر منفصل وآخر موزع على طول الخط . ولقد تبين أن خطوط التوزيع - على عكس خطوط النقل - قد تظهر أطيافا مختلفة للتردد حسب عوامل الخط والتربة، بالإضافة إلى مصدر التشويش وبعد نقطة القياس عن المصدر.